

## CONSTRAINING PHOSPHORUS CHEMISTRY IN CARBON- AND OXYGEN-RICH CIRCUMSTELLAR ENVELOPES: OBSERVATIONS OF PN, HCP, AND CP

S. N. MILAM,<sup>1</sup> D. T. HALFEN,<sup>2</sup> E. D. TENENBAUM,<sup>2</sup> A. J. APPONI,<sup>3</sup> N. J. WOOLF,<sup>2</sup> AND L. M. ZIURYS<sup>2</sup>

Received 2007 August 7; accepted 2008 April 4

### ABSTRACT

Millimeter-wave observations of PN, CP, and HCP have been carried out toward circumstellar envelopes of evolved stars using the Arizona Radio Observatory (ARO). HCP and PN have been identified in the carbon-rich source CRL 2688 via observations at 1 mm using the Submillimeter Telescope (SMT) and 2–3 mm with the Kitt Peak 12 m. An identical set of measurements were carried out toward IRC +10216, as well as observations of CP at 1 mm. PN was also observed toward VY Canis Majoris (VY CMa), an oxygen-rich supergiant star. The PN and HCP line profiles in CRL 2688 and IRC +10216 are roughly flat topped, indicating unresolved, optically thin emission; CP, in contrast, has a distinct “U” shape in IRC +10216. Modeling of the line profiles suggests abundances, relative to H<sub>2</sub>, of  $f(\text{PN}) \sim (3\text{--}5) \times 10^{-9}$  and  $f(\text{HCP}) \sim 2 \times 10^{-7}$  in CRL 2688, about an order of magnitude higher than in IRC +10216. In VY CMa,  $f(\text{PN})$  is  $\sim 4 \times 10^{-8}$ . The data in CRL 2688 and IRC +10216 are consistent with LTE formation of HCP and PN in the inner envelope, as predicted by theoretical calculations, with CP a photodissociation product at larger radii. The observed abundance of PN in VY CMa is a factor of 100 higher than LTE predictions. In IRC +10216, the chemistry of HCP/CP mimics that of HCN/CN and suggests an N<sub>2</sub> abundance of  $f \sim 1 \times 10^{-7}$ . The chemistry of phosphorus appears active in both carbon- and oxygen-rich envelopes of evolved stars.

*Subject headings:* astrobiology — astrochemistry — line: identification — stars: abundances — stars: chemically peculiar — stars: individual (CRL 2688; IRC +10216; VY CMa)

### 1. INTRODUCTION

Phosphorus plays a major role in biochemistry, being relevant to replication, metabolism, and structure in living systems (Pasek & Lauretta 2005). Yet it is not a particularly prevalent element, with a cosmic abundance relative to hydrogen of  $\text{P}/\text{H} \sim 2.8 \times 10^{-7}$  (Grevesse & Sauval 1998), less than that of iron, magnesium, sodium, calcium, and aluminum. Despite this fact, phosphorus is a frequent constituent in iron meteorites, where its common form is an iron-nickel-phosphide compound called schreibersite ([Fe, Ni]<sub>3</sub>P). Because of its concentrated presence in these types of meteorites, there is some thought that phosphorus needed for living systems was brought to Earth via meteoritic impact (Pasek & Lauretta 2005; Maciá 2005).

The history of phosphorus in interstellar gas is far less certain. This element is thought to be formed in massive stars ( $M > 15 M_{\odot}$ ) during hydrostatic-shell C and Ne burning (Arnett 1996). It is released into the interstellar medium as these objects become supernovae. The rarity of high-mass stars has a direct effect on the low (solar) P abundance, as compared to other “biotic” elements such as C, N, and O (Maciá 2005), which are all formed in a larger stellar population. In diffuse clouds, gas-phase phosphorus has been found to have an abundance that is consistent with minimal depletion into a solid form, based on P II observations (Lebouteiller et al. 2005). In dense gas, on the other hand, large depletions have been claimed because the only phosphorus-bearing gas-phase molecule observed thus far has been PN (Ziurys 1987; Turner & Bally 1987; Turner et al. 1990). However,

it could be that phosphorus exists in other, as yet undiscovered, gaseous molecular forms.

In circumstellar envelopes, the state of phosphorus chemistry, until recently, has been similar to that in molecular clouds. CP was the only species observed, and it was only in one object, the carbon star IRC +10216 (Guélin et al. 1990). However, HCP has now been definitively detected in IRC +10216, and PN has been tentatively identified in this object as well, based on one clean and one blended transition (Agúndez et al. 2007). Furthermore, PN and PO have recently been observed in the shell of the oxygen-rich red supergiant, VY Canis Majoris (VY CMa; Ziurys et al. 2007; Tenenbaum et al. 2007). Thus, four phosphorus-bearing compounds have now been identified in circumstellar gas.

Here we present observations of phosphorus-bearing molecules in another circumstellar source, the carbon-rich post-asymptotic giant branch (AGB) star CRL 2688. PN and HCP have been conclusively detected in this object. An additional transition of PN has also been observed in IRC +10216, confirming the presence of this species toward this star, as well as several lines of HCP. (The HCP data were discovered independently of Agúndez et al. [2007], and were in preparation for submission when their detection was published.) Several transitions of PN in VY CMa and CP in IRC +10216 have been measured as well for comparison. In this paper we present our observations, derive molecular abundances, and discuss their implications for phosphorus chemistry in circumstellar envelopes.

### 2. OBSERVATIONS

The measurements were conducted during the period 2006 October through 2007 June at 1, 2, and 3 mm using the facilities of the Arizona Radio Observatory (ARO): the Kitt Peak 12 m and Submillimeter Telescope (SMT) at Mount Graham, Arizona. The 1 mm observations were carried out at the SMT with a dual-polarization ALMA Band 6 receiver system employing sideband-separating mixers with an image rejection of typically 15–20 dB. The back end was a 2048 channel 1 MHz filter bank, used in

<sup>1</sup> SETI Institute, NASA Ames Research Center, MS 245-6, Moffett Field, CA 94035-1000; stefanie.n.milam@nasa.gov.

<sup>2</sup> Department of Chemistry, Department of Astronomy, NASA Astrobiology Institute, Steward Observatory, The University of Arizona, 933 North Cherry Avenue, Tucson, AZ 85721; halfendt@as.arizona.edu, emilyt@as.arizona.edu, nwoolf@as.arizona.edu, lziurys@as.arizona.edu.

<sup>3</sup> GEOST 7526 North Cholla Boulevard, Tucson, AZ 85741; aaponi@gmail.com.

TABLE 1  
OBSERVATIONS OF PHOSPHORUS SPECIES TOWARD CIRCUMSTELLAR ENVELOPES

Source	Molecule	Transition	Frequency (MHz)	$\eta_b$ or $\eta_c^a$	$\theta_b$ (arcsec)	$T_R$ (K)	$\Delta V_{1/2}$ (km s <sup>-1</sup> )	$V_{LSR}$ (km s <sup>-1</sup> )	$\int T_R dV$ (K km s <sup>-1</sup> )
CRL 2688 <sup>b</sup>	PN	$J = 2 \rightarrow 1$	93979.8	0.88	67	$0.003 \pm 0.002$	$25.5 \pm 6.4$	$-36.8 \pm 6.2$	0.061
		$J = 3 \rightarrow 2^c$	140967.8	0.76	44	$\sim 0.007$	$\sim 36$	$\sim -38$	0.118
		$J = 5 \rightarrow 4$	234935.7	0.78	32	$0.009 \pm 0.005$	$32.0 \pm 2.6$	$-37.4 \pm 2.6$	0.253
	HCP	$J = 4 \rightarrow 3$	159802.6	0.72	39	$0.012 \pm 0.006$	$29.5 \pm 3.8$	$-34.0 \pm 3.8$	0.354
		$J = 6 \rightarrow 5$	239693.8	0.78	31	$0.019 \pm 0.009$	$35.0 \pm 2.5$	$-35.9 \pm 2.5$	0.463
		$J = 7 \rightarrow 6$	279634.7	0.78	27	$0.028 \pm 0.010$	$28.9 \pm 3.2$	$-34.4 \pm 3.2$	0.758
IRC +10216 <sup>d</sup>	PN	$J = 2 \rightarrow 1$	93979.8	0.88	67	$0.007 \pm 0.001$	$28.7 \pm 6.4$	$-27.5 \pm 6.4$	0.177
		$J = 3 \rightarrow 2^c$	140967.8	0.76	44	$\sim 0.011$	$\sim 34$	$\sim -24$	0.221
		$J = 5 \rightarrow 4$	234935.7	0.78	32	$0.010 \pm 0.003$	$29.4 \pm 2.6$	$-27.3 \pm 2.6$	0.229
	HCP	$J = 4 \rightarrow 3$	159802.6	0.72	39	$0.010 \pm 0.003$	$24.5 \pm 3.8$	$-26.9 \pm 3.8$	0.233
		$J = 5 \rightarrow 4$	199749.4	0.78	38	$0.010 \pm 0.005$	$\sim 27$	$\sim -27$	0.241
		$J = 6 \rightarrow 5$	239693.8	0.78	31	$0.021 \pm 0.005$	$27.5 \pm 2.2$	$-26.6 \pm 2.2$	0.549
		$J = 7 \rightarrow 6$	279634.7	0.78	27	$0.028 \pm 0.008$	$27.9 \pm 2.1$	$-27.1 \pm 2.1$	0.760
	CP	$N = 5 \rightarrow 4$	...	...	...	...	...	...	...
		$J = 5.5 \rightarrow 4.5^c$	238856.5	0.78	32	$\sim 0.012$	$\sim 38$	$\sim -27$	0.500
		$J = 4.5 \rightarrow 3.5$	238303.1	0.78	32	$0.006 \pm 0.002$	$27.6 \pm 5.0$	$-27.2 \pm 2.5$	0.197
VY CMa <sup>e</sup>	PN	$J = 3 \rightarrow 2$	140967.8	0.76	44	$0.003 \pm 0.001$	$\sim 40$	$18.5 \pm 8.5$	0.120
		$J = 5 \rightarrow 4$	234935.7	0.78	32	$0.012 \pm 0.004$	$37.1 \pm 5.1$	$16.7 \pm 5.1$	0.473
		$J = 6 \rightarrow 5$	281914.1	0.78	27	$0.017 \pm 0.006$	$34.1 \pm 4.2$	$18.6 \pm 4.2$	0.487

NOTE.—All data measured with the SMT except the  $J = 2 \rightarrow 1, 3 \rightarrow 2$  lines of PN and the  $J = 4 \rightarrow 3$  line of HCP, which were observed with the ARO 12 m telescope.

<sup>a</sup>  $\eta_b$  and for SMT measurements and  $\eta_c$  and for 12 m data.

<sup>b</sup>  $\alpha = 21^{\text{h}}00^{\text{m}}20.0^{\text{s}}$ ,  $\delta = 36^{\circ}29'44''$  (B1950.0).

<sup>c</sup> Blended feature (see text).

<sup>d</sup>  $\alpha = 09^{\text{h}}45^{\text{m}}14.8^{\text{s}}$ ,  $\delta = 13^{\circ}30'40''$  (B1950.0).

<sup>e</sup>  $\alpha = 07^{\text{h}}20^{\text{m}}54.7^{\text{s}}$ ,  $\delta = -25^{\circ}40'12''$  (B1950.0).

parallel ( $2 \times 1024$ ) mode. The temperature scale at the SMT is  $T_A^*$ ; radiation temperature is then defined as  $T_R = T_A^*/\eta_b$ , where  $\eta_b$  is the main-beam efficiency. The 2 and 3 mm observations were conducted at the ARO 12 m using dual-polarization SIS mixers, operated in single-sideband mode with the image rejection  $\geq 20$  dB. Filter banks with 512 channels of 1 and 2 MHz resolutions were used simultaneously in parallel mode for the measurements, along with an autocorrelator with 782 kHz resolution. The intensity scale of the 12 m is the chopper-wheel corrected antenna temperature,  $T_R^*$ , including forward spillover losses, which is converted to radiation temperature by  $T_R = T_R^*/\eta_c$ , where  $\eta_c$  is the corrected beam efficiency. Data were taken in beam-switching mode with a subreflector throw of  $\pm 2'$ . Pointing and focus was monitored regularly by observations of nearby planets and quasars. Source coordinates, rest frequencies, telescope efficiencies, and beam sizes are given in Table 1.

### 3. RESULTS

The data obtained for CRL 2688 are presented in Figure 1. As shown, three rotational transitions were detected individually for HCP and PN toward this object. The  $J = 2 \rightarrow 1$  and  $3 \rightarrow 2$  lines of PN and the  $J = 4 \rightarrow 3$  transition of HCP were measured at the ARO 12 m, while the  $J = 6 \rightarrow 5$  and  $7 \rightarrow 6$  lines of HCP, as well as the  $J = 5 \rightarrow 4$  transition of PN, were observed at the SMT. As shown in Table 1, all features have local standard of rest (LSR) velocities in the range  $-34$  to  $-37$  km s<sup>-1</sup>, and line widths of  $\sim 35$  km s<sup>-1</sup>, typical parameters for CRL 2688 (e.g., Sopka et al. 1989; Young et al. 1992). The intensities are also consistent among the transitions. The HCP line profiles are roughly flat topped with evidence of a slight U shape, with stronger emission on the blueshifted side. This profile indicates unresolved, or partially resolved, optically thin emission. Observations of other molecules in CRL 2688 suggest a roughly spherical, AGB “remnant” flow of  $\sim 20''$ – $30''$  (Nguyen-Q-Rieu et al. 1984; Fukasaku et al.

1994; Highberger et al. 2003). The three transitions of HCP were measured with a beam size of  $\leq 39''$ , consistent with the extent of the remnant wind. Slight asymmetries are also present in line profiles from species arising in this flow, such as NaCl, NH<sub>3</sub>, and HC<sub>7</sub>N. Some of these asymmetries may result from the additional outflows present in CRL 2688, caused by an erratic, second phase of mass loss, which distorts the remnant AGB wind (e.g., Cox et al. 1997, 2000). The PN profiles are also flat topped in shape, although there is again evidence of a U in the  $J = 5 \rightarrow 4$  line, observed with the smallest beam of  $32''$ . The  $J = 3 \rightarrow 2$  transition of PN is unfortunately blended with <sup>30</sup>SiC<sub>2</sub> at 140956.2 MHz, with the  $J_{K_a, K_c} = 9_{3,6} \rightarrow 8_{3,5}$  transition of NaCN nearby at 140937.8 MHz.

In Figure 2, the same transitions of PN and HCP are shown for IRC +10216. The  $J = 3 \rightarrow 2$  transition of PN is contaminated by <sup>30</sup>SiC<sub>2</sub>, as in CRL 2688, but the  $J = 5 \rightarrow 4$  line is clean and confirms the presence of this species in IRC +10216. The LSR velocities and line widths found for these molecules are characteristic of this object (see Table 1; Cernicharo et al. 2000). The data from this source display the classic, flat-topped profile, suggesting that the emission is unresolved and optically thin. Agúndez et al. (2007) found slight U shapes in corresponding HCP spectra obtained with the IRAM 30 m telescope. These authors derived a source of roughly  $12''$ – $30''$ , consistent with the ARO beam sizes at these frequencies for unresolved emission.

Figure 3 displays the  $J = 3 \rightarrow 2, 5 \rightarrow 4,$  and  $6 \rightarrow 5$  transitions of PN toward VY CMa. All three lines of this molecule appear to exhibit somewhat triangular line profiles, likely coming from an ellipsoidal wind that is elongated in the plane of the sky (see Ziurys et al. 2007). PN is the first phosphorus-bearing species identified in an oxygen-rich, as opposed to carbon-rich, envelope. The initial detection of phosphorus nitride in this source was mentioned briefly in Ziurys et al. (2007), where the  $J = 5 \rightarrow 4$  spectra was presented.

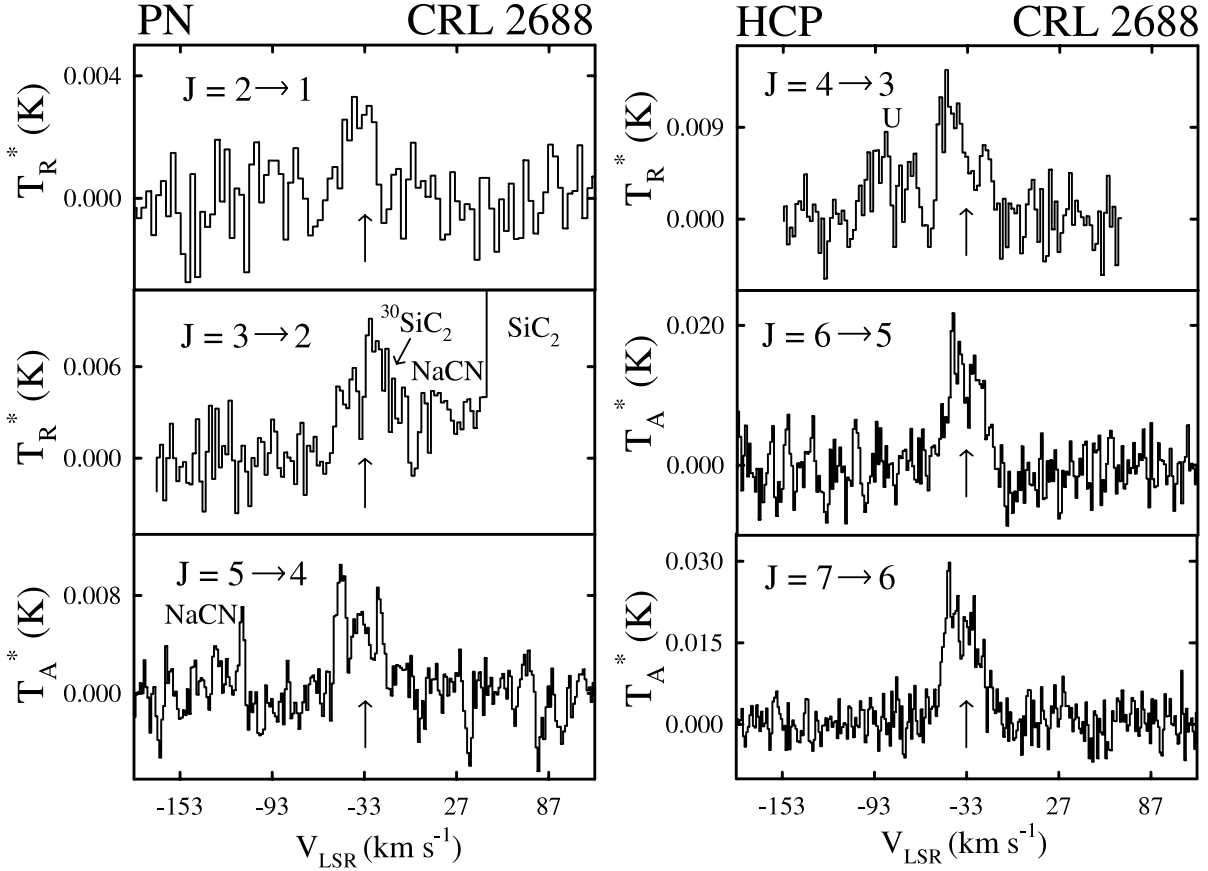


FIG. 1.—Spectra obtained for PN and HCP toward CRL 2688, using the ARO 12 m and SMT telescopes. *Right:*  $J = 4 \rightarrow 3$ ,  $6 \rightarrow 5$ , and  $7 \rightarrow 6$  transitions of HCP at 160, 240, and 280 GHz, which all display a slightly asymmetric U shape. *Left:*  $J = 2 \rightarrow 1$ ,  $3 \rightarrow 2$ , and  $5 \rightarrow 4$  transitions of PN at 94, 141, and 235 GHz. The  $J = 3 \rightarrow 2$  line of PN is contaminated by  $^{30}\text{SiC}_2$ , but the other two transitions are fairly flat topped, considering the signal-to-noise ratios. The PN  $J = 2 \rightarrow 1$  and  $J = 3 \rightarrow 2$ , as well as the HCP  $J = 4 \rightarrow 3$  lines, were obtained with the 12 m telescope, while the other spectra were measured at the SMT. All spectra were obtained with 1 MHz resolution. These measurements are clear evidence that these two phosphorus-bearing compounds are present toward CRL 2688.

For comparison, observations of the  $N = 5 \rightarrow 4$  lines of CP were also carried out toward IRC +10216; see Figure 4. This radical was originally detected in this source by Guélin et al. (1990), who measured several transitions. In Figure 4, the two fine-structure components of the  $N = 5 \rightarrow 4$  transition are shown. Each component consists of two hyperfine lines, but these are separated at most by 1.5 channels in the resolution displayed, and therefore do not affect the line shape. While the  $J = 5.5 \rightarrow 4.5$  feature is blended with the spin-rotation doublets of  $^{13}\text{CCCCH}$  (*top panel*), the  $J = 4.5 \rightarrow 3.5$  component is uncontaminated (*bottom panel*), and appears to be somewhat U shaped. Guélin et al. (1990) had suggested that this line was flat topped, but the signal-to-noise ratio is better in the current data shown here. Additional observations would help clarify this issue. If real, the U shape would again indicate a resolved, optically thin distribution and hence a source size of  $\sim 32''$ .

A complete summary of line parameters for all spectra is given in Table 1. These values include the measured main-beam brightness temperature, the FWHM line width, the LSR velocity, and the integrated intensity.

#### 4. ANALYSIS

##### 4.1. Circumstellar Radiative Transfer Code

In order to establish molecular abundances and spatial distributions, the radiative transfer code of Bieging & Tafalla (1993) was used. In this model, a set of statistical equilibrium equations are solved for populating rotational levels of a given molecule

assuming a spherically expanding circumstellar shell. Input parameters necessary for the modeling are distance to the object, outflow velocity, mass-loss rate, and temperature and density profiles. The gas temperature profile was modeled

$$T_{\text{kin}} = T_{\text{kin}0} \left( \frac{r}{r_{\text{kin}0}} \right)^{-0.7}. \quad (1)$$

The initial temperature,  $T_{\text{kin}0}$ , was assumed to be the effective temperature of the star and  $r_{\text{kin}0}$  was defined as the stellar radius. The exponent value of  $-0.7$  was chosen on the basis of other profiles from evolved stars (see Kemper et al. 2003; Keady et al. 1988). A density distribution dependence of  $r^{-2}$  was used for all model calculations, and the outflow velocity was established individually from the line profiles for a given species. Collisional cross sections for PN have been recently calculated by Tobola et al. (2007) and were incorporated into the model. Cross sections for HCP or CP are not known; thus, values for HCN and PN were used, respectively.

The model was used to reproduce the observed line profiles by varying two parameters: the molecular abundance relative to  $\text{H}_2$  and the radial source distribution. Both Gaussian and shell distributions were considered. For the Gaussian model, the expression describing the abundance distribution is given by

$$f(r) = f(X) e^{-(r/r_{\text{cfold}})^2}, \quad (2)$$

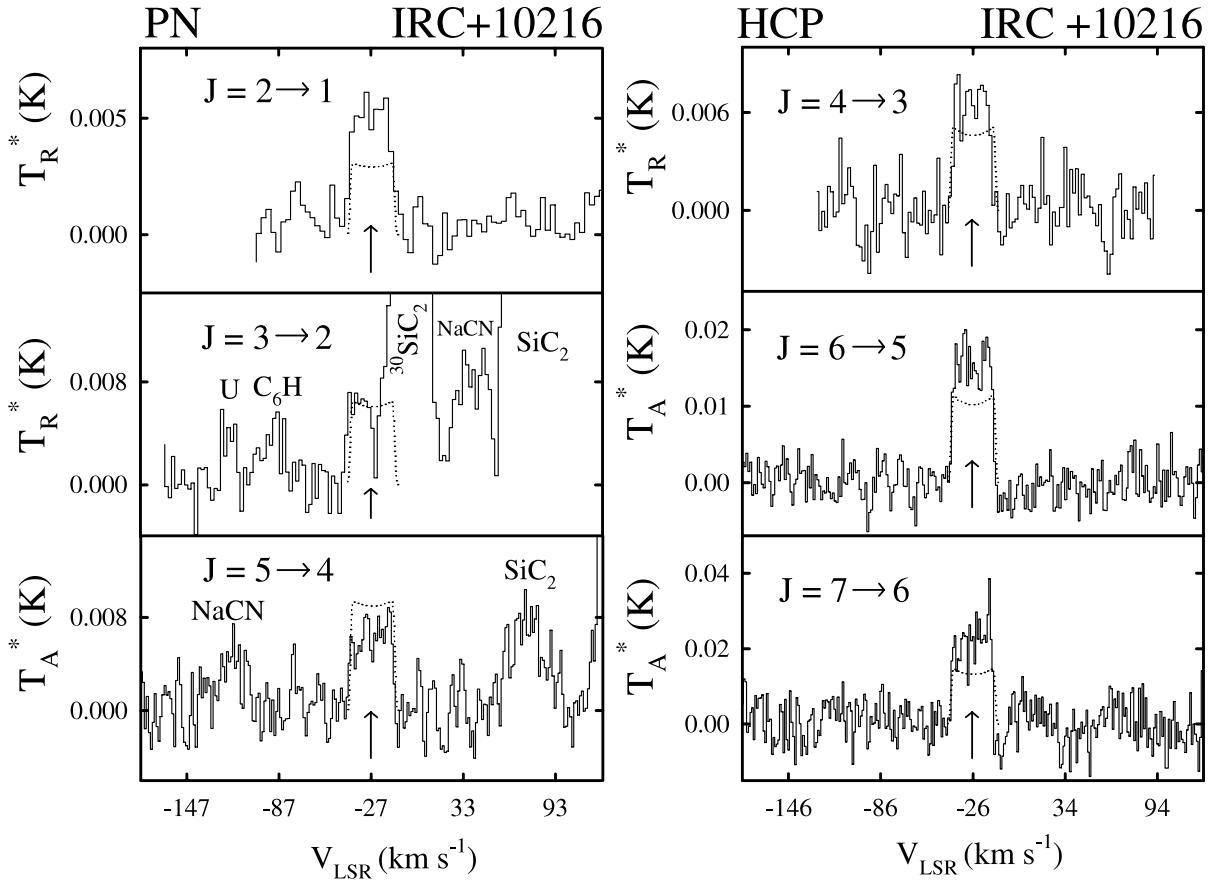


FIG. 2.—Set of spectra identical to that in Fig. 1, but observed toward IRC+10216. In this source, all lines display a flat-topped profile indicating optically thin, unresolved emission. The  $J = 3 \rightarrow 2$  line of PN (left) appears as a shoulder on the  $^{30}\text{SiC}_2$  feature. All data were taken with 1 MHz resolution. The model fits are shown by the dashed lines on the spectra.

where  $f(X)$  is the central abundance of a specific molecule and  $r_{\text{efold}}$  is the radius where the abundance decreases by  $1/e$ . For the shell distribution, the abundance function is

$$f(r) = f(X)e^{-[(r-r_{\text{max0}})/r_{\text{efold}}]^2}. \quad (3)$$

In this case,  $f(X)$  is the maximum abundance of the specified species,  $r_{\text{max0}}$  is the corresponding radius, and  $r_{\text{efold}}$  is the distance from  $r_{\text{max0}}$  where the abundance decreases by  $1/e$ . Three rotational transitions per molecule were simultaneously fit in most cases in order to constrain the model variables, except in the case of severe line contamination. When available, additional spectra from the literature were incorporated into the modeling.

The model fit for each source was determined by visual inspection. For the individual molecules in each envelope, the source distribution was successively varied in increments of  $5''$  and the abundance adjusted to obtain the best match to the observed spectrum.

The dipole moments used for PN, HCP, and CP were 2.75, 0.39, and 0.86 D, respectively (Pickett et al. 1998; Müller et al. 2005; Rohlffing & Almlöf 1988). Einstein  $A$ -coefficients were derived using these values and the appropriate dipole matrix element. Energy levels were calculated from the individual molecular rotational constants, which are listed in the JPL catalog (Pickett et al. 1998).

#### 4.2. Modeling of Observed Sources

Because independent estimates of source sizes were available for IRC+10216, these data were modeled first. The fitting

parameters assumed for IRC+10216 were a mass-loss rate of  $3 \times 10^{-5} M_{\odot} \text{ yr}^{-1}$ , an effective stellar temperature of  $T_{\text{eff}} \sim 2320 \text{ K}$ , a stellar radius of  $R_{*} \sim 6.5 \times 10^{13} \text{ cm}$ , and a distance of 150 pc (Agúndez & Cernicharo 2006). A fit to eight observed profiles of HCP (1 transition ARO 12 m; 3 transitions SMT; 4 transitions IRAM) yielded an  $e$ -folding radius of  $2.5 \times 10^{16} \text{ cm}$  ( $\theta_s = 22''$ ), assuming a spherical geometry, and a fractional abundance relative to  $\text{H}_2$  of  $f \sim 3 \times 10^{-8}$ . For PN, three spectral profiles were fit ( $J = 2 \rightarrow 1$ , Guélin et al. [2000] and ARO 12 m;  $J = 5 \rightarrow 4$ , SMT), yielding a source radius of  $4 \times 10^{16} \text{ cm}$  ( $\theta_s \sim 36''$ ) for a spherical distribution and a fractional abundance of  $f \sim 3 \times 10^{-10}$ . Shell geometries were also attempted in the analysis of the HCP and PN profiles, but were not as successful in reproducing these spectra. In the case of CP, only one transition could be reliably modeled: the  $J = 4.5 \rightarrow 3.5$  component of the  $N = 5 \rightarrow 4$  line. The other lines of CP observed in this work or by Guélin et al. (1990) were contaminated. In this case, both the IRAM and SMT data were modeled with a shell distribution. The shell source is consistent with the predictions of Agúndez et al. (2007) and the U shape observed at the SMT. The best fit to the two data sets suggests that CP arises from a shell approximately  $4 \times 10^{16} \text{ cm}$  wide ( $18''$  wide), with a peak abundance of  $f \sim 1 \times 10^{-8}$  at a radius of  $\sim 3 \times 10^{16} \text{ cm}$  ( $r \sim 13''$ ). The modeled spectra for all three molecules are overlaid on the observed lines in Figures 2 and 3.

For CRL 2688, the model parameters employed in the analysis are a distance of 1000 pc,  $R_{*} \sim 9 \times 10^{12} \text{ cm}$ ,  $T_{\text{eff}} \sim 6500 \text{ K}$ , and a mass-loss rate of  $1.7 \times 10^{-4} M_{\odot} \text{ yr}^{-1}$  (Skinner et al. 1997; Truong-Bach et al. 1990). The spectra for both PN and HCP were







# CONSTRAINING PHOSPHORUS CHEMISTRY IN CARBON- AND OXYGEN-RICH CIRCUMSTELLAR ENVELOPES: OBSERVATIONS OF PN, HCP, AND CP

S. N. Milam,<sup>1</sup> D. T. Halfen,<sup>2</sup> E. D. Tenenbaum,<sup>2</sup> A. J. Apponi,<sup>3</sup> N. J. Woolf,<sup>2</sup> and L. M. Ziurys<sup>2</sup>

Received 2007 August 7; accepted 2008 April 4

## ABSTRACT

Millimeter-wave observations of PN, CP, and HCP have been carried out toward circumstellar envelopes of evolved stars using the Arizona Radio Observatory (ARO). HCP and PN have been identified in the carbon-rich source CRL 2688 via observations at 1 mm with the Submillimeter Telescope (SMT) and 3 mm with the Kitt Peak 12 m. An identical set of measurements were carried out toward IRC +10216, as well as observations of CP